EUROPHYSICS LETTERS 1 October 2001

Europhys. Lett., **56** (1), pp. 112–118 (2001)

High-resolution X-ray emission and absorption study of the B $2p$ valence band electronic structure of MgB_2

C. McGuinness[1], K. E. Smith[1], S. M. Butorin[2], J. H. Guo[2], J. Nordgren[2], T. Vogt[3], G. Schneider[3], J. Reilly[3], J. J. Tu[3], P. D. Johnson[3] and D. K. Shuh[4]

[1] *Department of Physics, Boston University*
590 Commonwealth Avenue, Boston, MA 02215, USA
[2] *Department of Physics, Uppsala University - Box 530, 75121 Uppsala, Sweden*
[3] *Department of Physics, Brookhaven National Laboratory - Upton, NY 11973, USA*
[4] *Chemical Sciences Division, Lawrence Berkeley National Laboratory*
Berkeley, CA 94720, USA

(received 30 April 2001; accepted in final form 6 July 2001)

PACS. 74.25.Jb – Electronic structure.
PACS. 78.70.Dm – X-ray absorption spectra.
PACS. 78.70.En – X-ray emission spectra and fluorescence.

Abstract. – The occupied and unoccupied valence band states of MgB_2 have been studied using high-resolution soft X-ray emission and soft X-ray absorption spectroscopies. In particular, the B $2p$ partial density of states was measured near the Fermi level. The states at the Fermi edge are identified by comparison to calculation as being of B $2p_{xy}$ origin. Resonant inelastic X-ray scattering indicates the existence of low-energy excitations at the B $1s$-edge absorption threshold.

The discovery of superconductivity in MgB_2 with a critical temperature of $T_c = 39$ K has prompted extensive experimental and theoretical studies of this material [1]. Much of this interest is motivated by the realization that the measured superconducting transition temperature is close to the suggested theoretical limit for electron-phonon–mediated superconductivity [2]. Studies of the boron isotope effect [3] show behavior consistent with a phonon-mediated Bardeen-Cooper-Schrieffer (BCS) superconducting mechanism [4]. Inelastic neutron scattering measurements of the phonon density of states in $Mg^{11}B_2$ have resulted in further confirmation that a conventional phonon mechanism can explain the observed superconductivity with a moderately strong electron-phonon coupling [5]. Tunneling results indicate s-wave superconductivity [6–8]. Numerous electronic structure calculations for MgB_2 have been performed using extensions to the local density (LDA) approximation formalism [9–15]. The electronic structure of MgB_2 is predicted to show many similarities to graphite, in particular the formation of strong σ bonds by the planar sp^2 electrons and the location of the remaining valence electrons in non-bonding (p_z) π states. These band-structure calculations are all in general agreement with each other and show the B $2p_{xy}$ bands intersecting the Fermi level,

E_F. One calculation employing the linearized augmented plane-wave (LAPW) method has emphasized how the attractive potential of the Mg^{2+} between the B_2 layers results in a $\sigma \rightarrow \pi$ charge transfer via lowering of the π bands which drives the hole doping of the σ bands [12]. This hole doping, or hole pocket in the σ band, together with both the high density of states at E_F, and the very strong deformation potential of the σ bands from the bond stretching modes, are thought to be some of the specific features of MgB_2 that help give rise to such a remarkable T_c. Apart from the conventional BCS electron-phonon mechanism, an original approach to superconductivity in MgB_2 has been put forward based upon a "hole-undressing theory" [16–18].

Despite the high level of activity, spectroscopic studies of the bulk electronic structure of MgB_2 remain scarce. While angle-resolved photoemission spectroscopy is a powerful probe of electronic structure in solids [19, 20], it is very surface sensitive, and can be applied only with difficulty to powder, pressed-pellet, or sintered samples, such as those presently available for MgB_2 [21, 22]. In contrast, since it is not surface sensitive, synchrotron radiation-excited soft X-ray emission (SXE) spectroscopy is an ideal probe of the bulk electronic structure of multi-elemental materials not available in large single-crystal form [23]. Since the emission is governed by dipole selection rules, soft X-ray emission resulting from the creation of a core hole yields the density of states of the valence band resolved into orbital angular momentum components (*i.e.* the partial density of states (PDOS)) for that element. Complementary information to SXE concerning the empty density of states is obtained through soft X-ray absorption (SXA) spectroscopy [24].

We report here the results of a high-resolution SXE and SXA study of the valence band electronic structure of MgB_2. We have used SXE to directly measure the B $2p$ valence band PDOS, and have used SXA for equivalent measurements of the conduction band. Our results are directly compared to calculations. We find good agreement with the calculations, and that the boron states at E_F are largely of B p_{xy} origin. We performed a resonant inelastic X-ray scattering experiment by exciting the SXE close to the B $1s$ absorption threshold, and have observed low-energy electronic excitations. Our results are in broad agreement with contemporaneous synchrotron radiation-excited [25] and electron beam-excited SXE studies [26].

Two samples of MgB_2 were prepared and studied. The first was commercially available MgB_2 powder obtained from Alfa-Aesar which was mechanically compressed into a pellet. The surface of this sample was then prepared by scraping with a clean diamond file. The second sample was prepared by heating elemental Mg and B in a Ta ampule to 950 °C for 2 hours [3]. High-resolution powder diffraction data indicated Mg and MgO incorporated in this sample. The unit cell dimensions of the main phase MgB_2 ($a = 3.08592(1)$ Å and $c = 3.52119(3)$ Å) agree well with pure MgB_2 used in other experiments [13]. Resistivity measurements were carried out on this sintered pellet and clearly show a sharp superconducting transition at 39 K. This sample was also scraped with a clean diamond file giving rise to a metallic-like surface prior to loading of the sample into the ultra-high vacuum chamber in which the measurements took place. Our SXE and SXA experiments were performed on undulator beamline 7.0 of the Advanced Light Source, Lawrence Berkeley National Laboratory; this beamline is equipped with a spherical grating monochromator [27]. Emission spectra were recorded using a Nordgren-type grazing-incidence grating spectrometer with a total energy resolution of ∼0.3 eV [23]. The resolution of the emission spectra was determined from both the nominal instrumental resolutions of the monochromator and spectrometer, respectively, and as measured directly from the observed width of the elastically scattered photon beam. Samples were mounted with their surface normal located in the horizontal scattering plane. The incidence angle of the photon beam was about 25° from the sample surface, with the emission spectrometer at 90° to the incident beam. Absorption spectra were recorded by

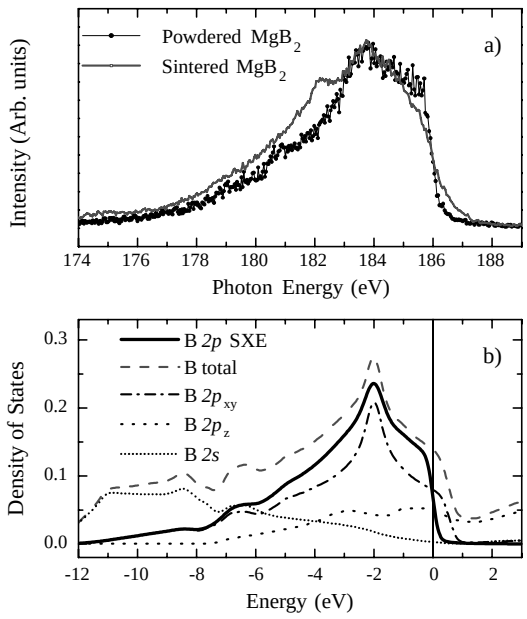

Fig. 1

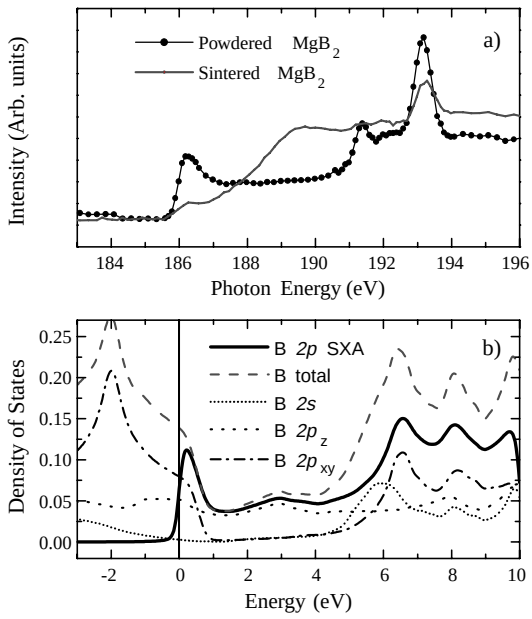

Fig. 2

Fig. 1 – a) SXE spectra taken with $h\nu_{\rm exc} = 209.4$ eV for the powdered MgB_2, and $h\nu_{\rm exc} = 215.89$ eV for the sintered sample. b) The calculated occupied B $2p$ PDOS, broadened to account for instrumental resolution and core-hole lifetime. Also shown are the total B PDOS and its orbital subcomponents the B $2s$, $2p_z$ and $2p_{xy}$ PDOS. The zero in energy is $E_{\rm F}$.

Fig. 2 – a) SXA spectra taken from the powdered and sintered MgB_2 sample. b) Calculated unoccupied B $2p$ PDOS broadened to account for instrumental resolution and core-hole lifetime. Also shown are the total B PDOS and its orbital subcomponents the B $2s$, $2p_z$ and $2p_{xy}$ PDOS. The zero in energy is $E_{\rm F}$.

measuring the total fluorescence yield (TFY) with normal incidence of the incoming radiation. The total energy resolution was approximately 0.2 eV. All experiments were performed with the samples at room temperature. Vacuum pressures during the measurements were below 5×10^{-9} Torr.

Figure 1a) presents the occupied B $2p$ PDOS from both the powdered and sintered MgB_2 samples as measured using SXE to a B $1s$ hole. Figure 1b) presents a calculation of the occupied PDOS. The calculated PDOS was computed within density functional theory using the full-potential linearized augmented plane-wave method FLAPW [28–31]. Further details of the basis set and lattice parameters used in these calculations can be found elsewhere [13]. Shown in fig. 1b) are the total B PDOS, and its sub-components due to the B $2s$, $2p_z$ and $2p_{xy}$ orbitals. Note in particular the PDOS of the B $2p_{xy}$ orbitals at $E_{\rm F}$ as the importance of these states for the superconductivity of MgB_2 has been pointed out by several authors [9, 12]. It is these states that participate in the sp^2 planar bonding similar to graphite, as noted earlier, and their two-dimensional character has been highlighted by calculations of the electronic structure under pressure [13]. For comparison with the experimental data the theoretical B total $2p$ PDOS was first convoluted by a Fermi function and then by a Lorentzian (0.07 eV) to simulate core-hole lifetime broadening and finally convoluted by a Gaussian (0.3 eV) to simulate the instrumental broadening. The overall agreement between the measured and

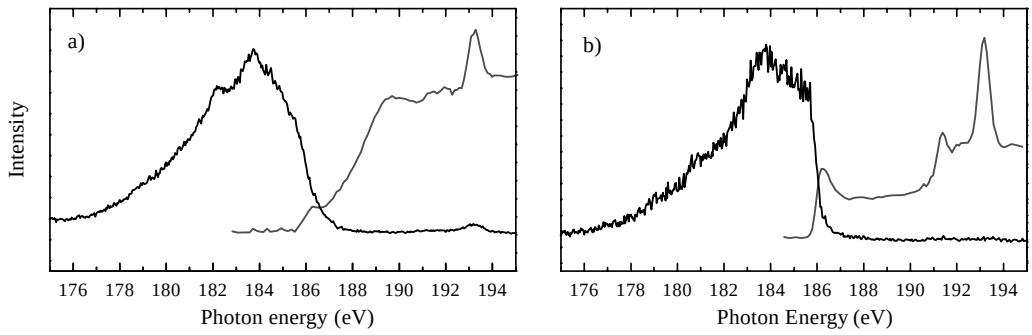

Fig. 3 – Comparison of measured B $2p$ occupied and unoccupied PDOS for the a) sintered MgB_2 sample and b) the powdered MgB_2 sample.

calculated PDOS is quite good. However there are clear differences between the SXE spectra from the powdered and sintered samples: most noticeably in the middle of the valence band, about 4 eV below E_F, but also in the emission very close to E_F.

The difference between the powder and sintered samples is also evident in their respective SXA spectra. Figure 2a) presents the SXA spectra recorded as the incident photon energy was swept through the B $1s$ absorption edge. The energy scale of the X-ray absorption spectra were calibrated by reference to the X-ray absorption spectrum of hexagonal-BN [32]. The SXA spectrum from the powdered sample clearly shows a sharp peak at the absorption threshold of 186.2 eV, followed by a second peak at 191.4 eV and a third intense feature at 193.2 eV. The SXA spectrum from the sintered sample also shows a clear absorption threshold at 186.2 eV, but as the photon energy increases, the absorption increases steadily to a broad shoulder at 189.5 eV. The absorption features observed in the SXA from the powdered sample at 191.4 eV and 193.2 eV are also visible in the spectrum from the sintered sample, although the feature at 191.4 eV is much less well defined. Figure 2b) shows the calculated unoccupied B $2p$ PDOS together with the total B PDOS and its orbital components. As with the B $2p$ PDOS calculation for the occupied states in fig. 1b), the calculated PDOS was convoluted with a Fermi function and then broadened to account for core-hole lifetime effects (0.07 eV) and instrument resolution (0.2 eV). The overall agreement between the experiment and calculation is quite good for the compressed powder sample of MgB_2, but less good for the sintered sample. The features of the absorption spectrum will be discussed further below. Note that the SXE and SXA spectra can be placed on the same energy scale through measurement of the elastically scattered photons. Figure 3 shows the full occupied and unoccupied states as measured for both the sintered (fig. 3a) and powdered (fig. 3b) samples.

The SXE spectra presented in fig. 1 were recorded with a photon excitation energy far above the B $1s$ absorption threshold. Under such circumstances, the spectra accurately reflect the elementally resolved PDOS. However, as the incident photon energy is varied through the absorption features identified in the SXA spectra of fig. 2, changes in the structure of the emission spectra are observed. Figure 4 presents a series of SXE spectra as a function of excitation energy from the powdered sample, while fig. 5 presents the equivalent set of spectra for the sintered sample. Elastic scattering is visible in both sets of spectra as the intense feature dispersing with excitation energy.

By comparison to the calculated B $2p$ PDOS, the threshold peak in the SXA spectra (fig. 2) can be identified as being due to transitions to empty B $2p_{xy}$ states. The second absorption feature seen at 191.4 eV is very similar in energy to that observed in h-BN [32]

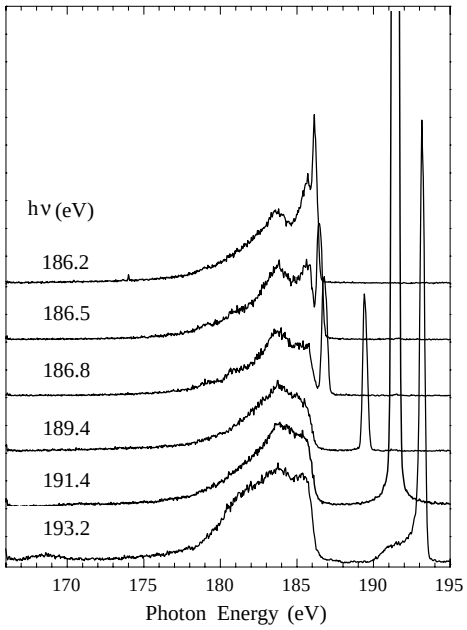

Fig. 4

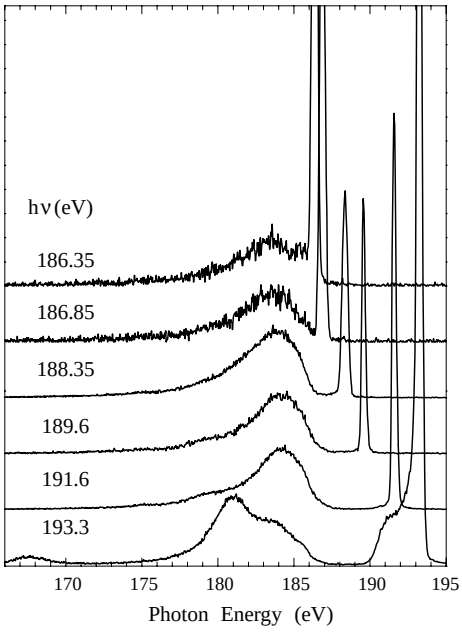

Fig. 5

Fig. 4 – SXE spectra as a function of photon excitation energy for the powdered MgB_2 sample.

Fig. 5 – SXE spectra as a function of photon excitation energy for the sintered MgB_2 sample.

although it should be noted that there is a wide variation in the literature of the energy given for this feature [32–35]. It can be seen that at this excitation energy, the magnitude of the elastic peak in the emission spectrum (fig. 4) is considerably enhanced. In *h*-BN the equivalent emission feature results from resonant fluorescence (spectator) emission from an excitonic state which corresponds to a normally unoccupied π^* antibonding state present when the boron in these systems is sp^2 bonded [35]. MgB_2 is also sp^2-bonded and thus also exhibits a π^* resonance feature accounting for the dramatic increase in the elastically scattered peak when on this resonance. The third prominent feature seen in the absorption spectrum from both samples occurs at 193.2 eV (fig. 2). It is notable that at this excitation energy, the emission spectra from both samples (figs. 4 and 5) show the elastically scattered peak to have structure on the low-energy side, corresponding to inelastic losses due to electronic excitations. Furthermore, the structure of the emission spectra is quite different than that observed far above threshold, with new emission features appearing at 167 eV and at 181 eV. These features are characteristic of boron oxide (B_2O_3) [36], and indicate some level of oxide contamination present in both of the MgB_2 samples. A contemporaneous SXE study has commented on the contribution of surface boron oxides and the possible degradation of MgB_2 surfaces exposed to air for long periods [25]. Our measurements indicate that surface boron oxides are more substantial in the sintered sample.

Soft X-ray emission measures the PDOS of the unperturbed system under the assumption that correlation effects, such as final-state interactions, are negligible, and SXE spectra depend little on the excitation energy if the core electron is excited to a delocalized state. However, when SXE spectra are measured with the excitation energy very close to an absorption edge, strong changes in the emission structure with variation of the excitation energy can

be observed. This may be interpreted as resonant inelastic X-ray scattering (RIXS), described by the second-order Kramers-Heisenberg scattering formula. We have recorded RIXS spectra from both MgB_2 samples, and have observed an energy loss from the elastically scattered peak at approximately 0.5–0.8 eV. This inelastic loss overlaps in energy with the normal emission from the B $2p$ PDOS. Typically the interpretation of such a feature in a transition metal oxide system would be as a RIXS feature due to *d-d* excitations [37,38]. By analogy, it is reasonable to interpret the losses in MgB_2 as being due to *p-p* transitions. As seen in previous calculations, the energy separation of the two $2p_{xy}$ σ bonding bands as they approach and cross the Fermi surface is of the order of 0.5 eV which can be heightened by the large deformation potential of the in-plane E_{2g}-boron stretching mode to as much as 1.5 eV [9, 12].

In conclusion, the measured B $2p$ PDOS of MgB_2 agrees well with the results of calculated electronic structure, particularly in the case of the compressed powder pellet. While exhibiting a superconducting transition as indicated by resistivity measurements, the SXE and SXA spectra from the sintered polycrystalline MgB_2 sample do not agree so readily with the theoretical results. This may be partly due to the presence of significant surface boron oxides. The low-energy excitations, which appear as losses off the elastically scattered incident photon energy that are observed at threshold, are proposed as being due to *p-p* excitations.

* * *

The Boston University program is supported in part by the US Department of Energy (DOE) under DE-FG02-98ER45680. The BNL program is supported in part by DE-AC02-98CH10886. Experiments were undertaken at the ALS, which is supported by the US DOE, Division of Materials Sciences under DE-AC03-76SF00098 at LBNL. The Uppsala University research is supported by NFR (the Swedish Natural Science Research Council) and the Göran Gustafsson Foundation for Research in Natural Sciences and Medicine. DKS is supported by the Chemical Sciences Division of the US DOE under contract DE-AC03-76SF00098 at LBNL. The support of the ALS for these experiments is gratefully acknowledged.

REFERENCES

[1] Nagamatsu J., Nakagawa N., Muranaka T. *et al.*, *Nature*, **410** (2001) 63.
[2] McMillan W. L., *Phys. Rev.*, **167** (1968) 331.
[3] Bud'ko S. L., Lapertot G., Petrovic C. *et al.*, *Phys. Rev. Lett.*, **86** (2001) 1877.
[4] Bardeen J., Cooper L. N. and Schrieffer J. R., *Phys. Rev.*, **108** (1957) 1175.
[5] Osborn R., Goremychkin E. A., Kolesnikov A. I. *et al.*, *Phys. Rev. Lett.*, **87** (2001) 017005.
[6] Rubio-Bollinger G., Suderow H. and Vieira S., *Phys. Rev. Lett.*, **86** (2001) 5582.
[7] Karapetrov G., Iavarone M., Kwok W. K. *et al.*, *Phys. Rev. Lett.*, **86** (2001) 4374.
[8] Sharoni A., Felner I. and Millo O., *Phys. Rev. B*, **63** (2001) 220508R.
[9] Kortus J., Mazin I. I., Belashchencko K. D. *et al.*, *Phys. Rev. Lett.*, **86** (2001) 4656.
[10] Belashchenko K. D., Schilfgaarde M. V. and Antropov V. P., cond-mat/0102290 Preprint, 2001.
[11] Satta G., Profeta G., Bernadini F. *et al.*, cond-mat/0102358 Preprint, 2001.
[12] An J. M. and Pickett W. E., *Phys. Rev. Lett.*, **86** (2001) 4366.
[13] Vogt T., Schneider G., Hriljac J. A. *et al.*, cond-mat/0102480 Preprint, 2001.
[14] Kong Y., Dolgov O. V., Jepsen O. *et al.*, *Phys. Rev. B*, **64** (2001) 020501R.
[15] Medvedeva N. I., Ivanovskii A. L., Medvedeva J. E. *et al.*, *Phys. Rev. B*, **64** (2001) 020502R.
[16] Hirsch J. E., *Phys. Lett. A*, **282** (2001) 392.
[17] Hirsch J. E. and Marsiglio F., cond-mat/0102479 Preprint, 2001.

[18] Hirsch J. E., *Phys. Rev. B*, **62** (2000) 14487.
[19] Kevan S. D., *Angle Resolved Photoemission* (Elsevier, Amsterdam) 1991.
[20] Smith K. E. and Kevan S. D., *Prog. Solid State Chem.*, **21** (1991) 49.
[21] Vasquez R. P., Jung C. U., Park M.-S. *et al.*, cond-mat/0103215 Preprint, 2001.
[22] Takahashi T., Sato T., Souma S. *et al.*, *Phys. Rev. Lett.*, **86** (2001) 4915.
[23] Nordgren J., Bray G., Cramm S. *et al.*, *Rev. Sci. Instrum.*, **60** (1989) 1690.
[24] Stöhr J., *NEXAFS Spectroscopy* (Springer, Berlin) 1992.
[25] Callcott T. A., Lin L., Woods G. T. *et al.*, cond-mat/0103593 Preprint, 2001.
[26] Kurmaev E. Z., Lyakhovskaya I. I., Kortus J. *et al.*, cond-mat/0103487 Preprint, 2001.
[27] Warwick T., Heimann P., Mossessian D. *et al.*, *Rev. Sci. Instrum.*, **66** (1995) 2037.
[28] Kohn W. and Sham L. J., *Phys. Rev. A*, **140** (1965) 1133.
[29] Hohenberg P. and Kohn W., *Phys. Rev. B*, **136** (1964) 864.
[30] Jansen H. J. F. and Freeman A. J., *Phys. Rev. B*, **30** (1984) 561.
[31] Wimmer E., Krakauer H., Weinert M. *et al.*, *Phys. Rev. B*, **24** (1981) 864.
[32] O'Brien W. L., Jia J., Dong Q. Y. *et al.*, *Phys. Rev. Lett.*, **70** (1993) 238.
[33] Jia J. J., Callcott T. A., Shirley E. L. *et al.*, *Phys. Rev. Lett.*, **76** (1996) 4054.
[34] Moscovici J., Loupias G., Parent P. *et al.*, *J. Phys. Chem. Solids*, **57** (1996) 1159.
[35] Carlisle J. A., Terminello L. J., Hudson E. A. *et al.*, *Appl. Phys. Lett.*, **67** (1995) 34.
[36] Muramatsu Y., Oshima M. and Kato H., *Phys. Rev. Lett.*, **71** (1993) 448.
[37] Kuiper P., Guo J. H., Sathe C. *et al.*, *Phys. Rev. Lett.*, **80** (1998) 5204.
[38] Butorin S. M., Guo J. H., Magnuson M. *et al.*, *Phys. Rev. B*, **54** (1996) 4405.